

Fabrication of zinc-aluminum layer double hydroxide thin films and their anionic adsorption performance

S. Laksee^a, W. Chitaka^b, K. Laohhasurayotin^c, C. Suwanchawalit^{b,*}

^a*Nuclear Technology Research and Development Center, Thailand Institute of Nuclear Technology (Public Organization), Nakhon Nayok, 26120 Thailand*

^b*Department of Chemistry, Faculty of Science, Silpakorn University, Nakorn Pathom, 73000 Thailand*

^c*National Nanotechnology Center (NANOTEC), National Science and Technology Development Agency (NSTDA), 111 Thailand Science Park, Phahonyothin Road, Khlong Nueng, Khlong Luang, Pathum Thani, Thailand 12120*

Layered double hydroxides (LDHs) are also known as hydrotalcite-like compounds or anionic clays. In this work, ZnAl-LDH films were prepared on aluminium (Al) plates by a hydrothermal technique using zinc nitrate solution as the precursors. ZnAl-LDHs films were characterized by SEM, EDX, XRD and FT-IR. The SEM analysis revealed that the ZnAl-LDH films with hierarchical nanoarchitectures on the surface of Al plates. EDX mapping and elemental analysis also showed that Zn, Al, and O dispersed uniformly on the aluminium substrates. XRD results were used to confirm the presence of ZnAl-LDH films as they appeared purely with the typical (003) and (006) peaks of LDH diffraction. The characteristic bands of bending vibrations due to the intercalating water, stretching vibration due to the overlapping signal of carbonate anion and nitrate anion were measured by FT-IR spectroscopy. The brucite structure also exhibited the OH-stretching vibration as well as the ZnO lattice vibration in the spectra. These ZnAl-LDH forms were evaluated for their removal performance against orange II dye solutions.

(Received October 9, 2021; Accepted January 27, 2022)

Keywords: LDHs, Zinc-aluminum layer double hydroxide, Hydrothermal technique, Anionic adsorption, Orange II dye

1. Introduction

Synthetic dyes are widely used in the textile industry. The release of liquid effluent pollutants from the coloring process leads to high quantities of dye wastewater [1, 2]. These colored effluents contain aromatic pollutants, making them non-biodegradable and carcinogenic for humans and the environment [3]. These colored effluents not only cover surface of waters and block the sunlight to reach the plant, but also cause consecutively the serious reduction of dissolved oxygen which makes the environmental problem worse to the aqua system. Various approaches have been developed to remove these pollutants in wastewater such as adsorption [4, 5], coagulation [6] and photocatalysis [7, 8]. Among these methods, adsorption is a suitable method to remove dye from the aqueous solution because it is an easy, fast, cheap and pollutant-free technique. Various absorbents, i.e. activated carbon [9], kaolin [10], bentonite [11] and layered double hydroxide [12-14] have been used in this technique.

Layered double hydroxides (LDHs) is a hydrotalcite-like compound or anionic clay having a sandwich structure composed of a cationic layer and an anionic interlayer. LDHs have been synthesized from various divalent ($M^{2+} = Mg^{2+}$, Zn^{2+} and Ni^{2+}) and trivalent cations ($M^{3+} = Al^{3+}$, Fe^{3+} and Cr^{3+}) in variable M^{2+}/M^{3+} mole ratios and accompanied by interlayer anions of diverse nature. It is well known that the general formula of layered double hydroxide is

* Corresponding author: suwanchawalit_c@su.ac.th
<https://doi.org/10.15251/DJNB.2022.171.127>

$[M_{1-x}^{2+}M_x^{3+}(\text{OH})_2]^{x+} A_{x/n}^{n-} \cdot m\text{H}_2\text{O}$, with A^{n-} as exchangeable anion interlayer [15-17]. The unique properties of LDHs, such as anion exchangeability, cation compatibility, pore size adjustability and the memory effect of their structure, show great removal efficiencies of contaminants.

In the present work, zinc-aluminum layer double hydroxide thin films (ZnAl-LDHs) grown on an aluminum plate were prepared via the hydrothermal method. The hydrothermal temperatures for preparing the ZnAl-LDHs-grown thin films on aluminum surface were investigated. The synthesized ZnAl-LDHs samples were characterized by various physical techniques such as X-ray diffraction spectrometry (XRD), scanning electron microscopy (SEM), and Fourier-transformed infrared spectroscopy (FT-IR). The adsorption properties of the as-prepared ZnAl-LDHs samples were tested using orange II dye (OII) as a model pollutant. A possible adsorption mechanism has been proposed.

2. Experimental

2.1. Materials

Aluminum plate (Al), ethanol ($\text{C}_2\text{H}_5\text{OH}$, Merck), sodium hydroxide (NaOH, Lobachemie), zinc (II) nitrate hexahydrate ($\text{Zn}(\text{NO}_3)_2 \cdot 6\text{H}_2\text{O}$, Lobachemie), nitric acid (HNO_3 , Merck) and orange II (OII, Sigma-Aldrich) were used to synthesize the zinc-aluminum layer double hydroxide thin films (ZnAl-LDHs). All chemicals and solvents were analytical grade and purified according to standard procedures.

2.2. Preparation of ZnAl-LDHs films

In this study, zinc-aluminum layer double hydroxide thin films (ZnAl-LDHs) grown on an aluminum plate were prepared via the hydrothermal method according to the following procedure, as shown Fig. 1. First, the aluminum plate (3 x 10 cm) was pretreated with ethanol to remove the impurities on the surfaces, then it was treated with 0.1 M sodium hydroxide (NaOH) to form tetrahydroxoaluminate ion ($[\text{Al}(\text{OH})_4]^-$) on the surface of aluminum plate, and then rinsed with distilled water. The pretreated aluminum plates were collected and dried at room temperature. The pH of 80 mL of 1.0 M zinc (II) nitrate hexahydrate ($\text{Zn}(\text{NO}_3)_2 \cdot 6\text{H}_2\text{O}$) was then adjusted to 2.0 by the addition of 0.1 M nitric acid (HNO_3). The resulting solution and the pre-treated aluminium plates were transferred to a hydrothermal autoclave reactor. The reactor was sealed in a conventional oven at various temperatures (120, 150, 200 and 250 °C). After 24 h, the resulting films of the ZnAl-LDHs on the aluminum plate were rinsed with deionized (DI) water and dried under ambient conditions.

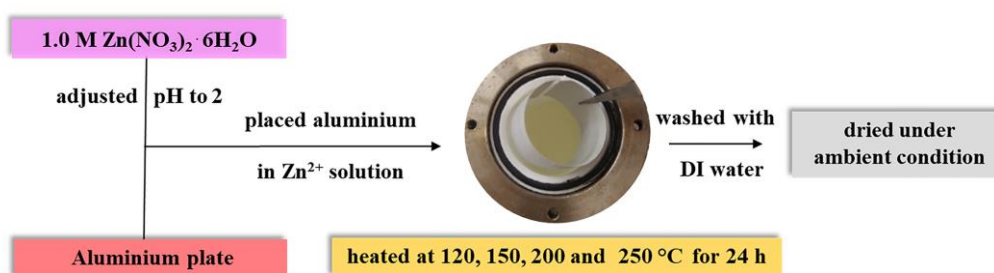


Fig. 1. Synthetic pathway of the ZnAl-LDHs films.

2.3. Characterization of ZnAl-LDHs

Studies on the morphology, chemical compositions, crystal structure and functional groups of ZnAl-LDHs were carried out using X-ray diffractometry (XRD), scanning electron microscopy (SEM), energy dispersive X-ray spectrometry (EDS), and Fourier transform infrared spectroscopy (FTIR). Briefly, the morphological characteristics and chemical compositions were investigated by

SEM and EDS (Hitachi S-3400). The crystal structures of the as-prepared ZnAl-LDHs samples were determined through XRD recorded in a Shimadzu 6100 X-ray diffractometer with Cu K α radiation (1.5406 Å) at 2θ from 5 to 40° with a scan rate of 2 °C/min. FT-IR spectra were obtained with a Nicolet 6700 spectrophotometer in the range of 400-4000 cm⁻¹ via attenuated total reflectance (ATR) to study the functional groups of newly prepared ZnAl-LDHs.

2.4. Adsorption studies

The adsorption properties of these samples were evaluated by the photodegradation of orange II (OII) dye in an aqueous solution. Four pieces of the newly prepared ZnAl-LDHs (1.00 x 5.00 cm) were placed in a 50 mL of orange II solution at a concentration of 200 and 600 ppm. To establish adsorption equilibrium, all samples were added to the dye aqueous solution for 24 h. Their absorbance was recorded at 485 nm using a Perkin Elmer UV-Vis spectrophotometer (Hewlett-Packard 8453). The removal efficiencies of the ZnAl-LDHs were calculated using equation (1).

$$\text{Removal efficiency (\%)} = ((C_0 - C_T) / C_T) \times 100 \quad (1)$$

where, C_0 is the initial concentration of OII, and C_T is the concentration of OII at time intervals.

3. Results and Discussion

3.1. Preparation and characterizations of ZnAl-LDHs

In this work, the ZnAl-LDHs films were successfully synthesized on the aluminum plate by hydrothermal method at various temperatures ranging from 120, 150, 200 and 250 °C to study the effect of temperature on the preparation of ZnAl-LDHs films. Under the prepared condition, the solution comprising zinc ions (Zn²⁺) and aluminum ions (Al³⁺) were used to co-precipitate particles in bulk solution on the aluminum plate to form ZnAl-LDHs [18, 19].

The characterizations of the samples were carried out in the following sections, including surface morphology, chemical compositions, crystal structure determination, functional groups and dye removal efficiency. After synthesis, the photos of ZnAl-LDHs films on the aluminum plate were taken with camera (model Oppo mirror 5) shown in Fig. 2. As can be observed, the ZnAl-LDHs films of uniform density were grown over the whole area of the Al plate surface consisting of many interconnecting nanosheets. The formations of white crystals on the Al plate gradually increased with increasing reaction temperature, resulting in the greater generation of ZnAl-LDHs films on the Al plate with their *ab* plane perpendicular to the Al plate (*c*-axis parallel to the Al substrate), consistent with a previous study [18, 20].

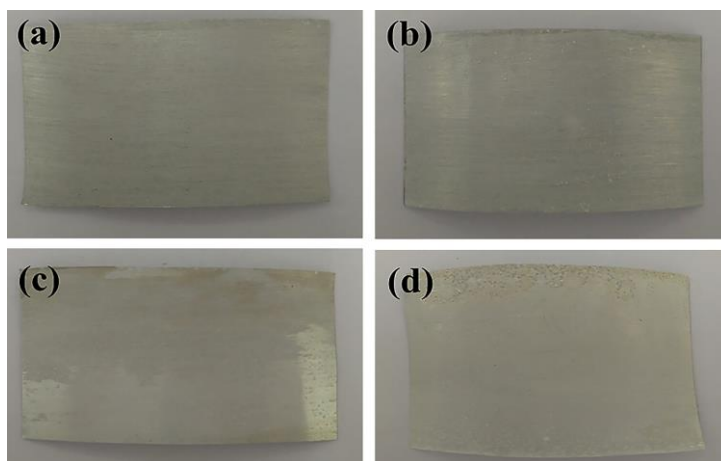


Fig. 2. The photographic images of the ZnAl-LDHs films coated on the Al plate by hydrothermal method at (a) 120, (b) 150, (c) 200 and (d) 250 °C.

The morphological characteristics of the Al plates and the ZnAl-LDHs films on the Al plate at various temperatures were observed by SEM as illustrated in Fig. 3. The surface of the uncoated Al plate included many grooves and ripples formed during the surface preparation steps (Fig. 3a), whereas the Al plate coated with ZnAl-LDHs films at various temperatures revealed ZnAl-LDH films with hierarchical nanoarchitectures fabricated on the surface of Al, showing distinctive surface morphologies.

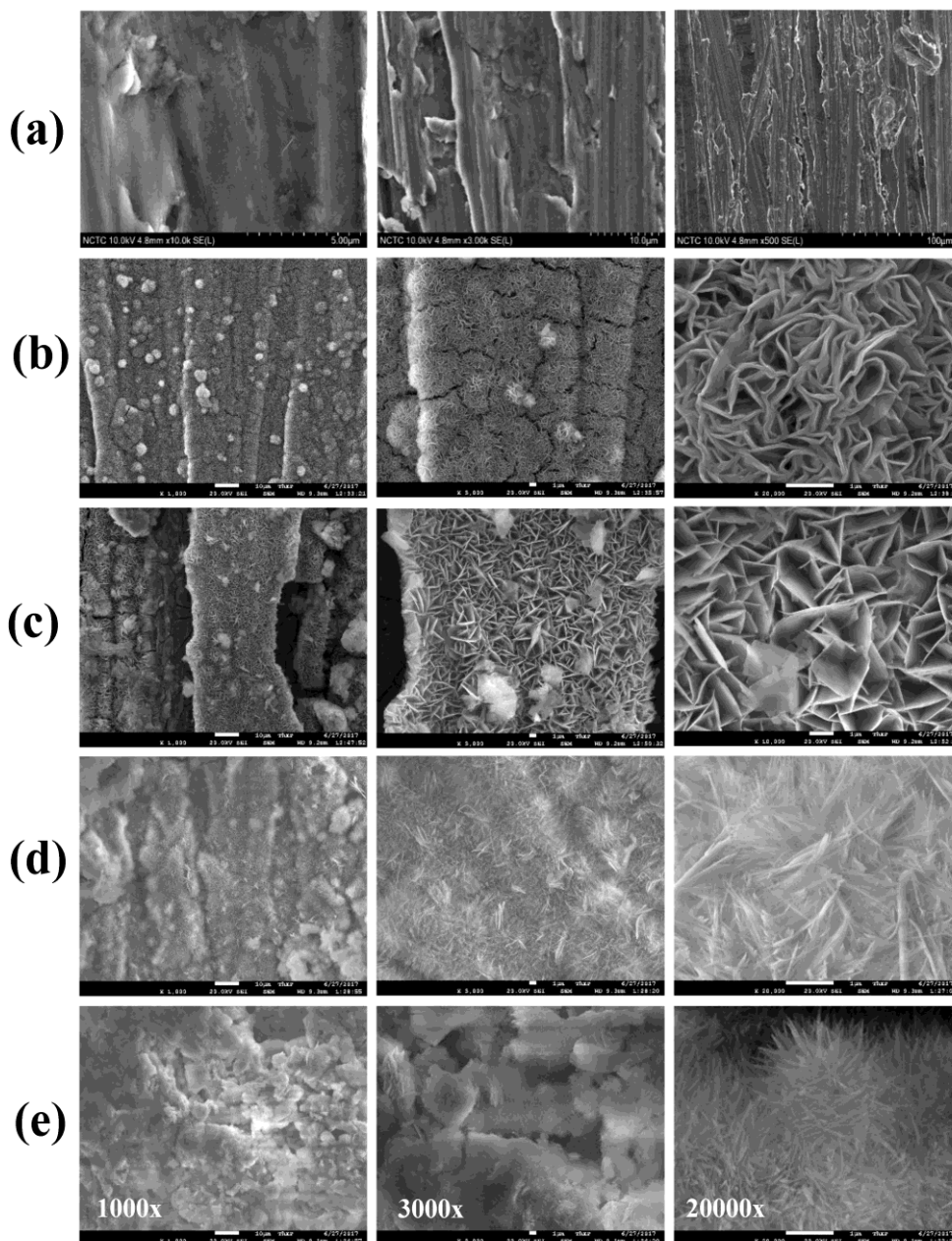


Fig. 3. SEM images of (a) the Al plates, and the ZnAl-LDHs on the Al plate via the hydrothermal process at (b) 120, (c) 150, (d) 200 and (e) 250 °C.

The SEM images of the ZnAl-LDHs films at different scales from μm to nm and at different magnifications were obtained. After synthesis, the ZnAl-LDHs coated on the Al plate at 120 and 150 °C (Fig. 3b-c) appeared as thin films possessing hierarchical nanoarchitectures. Its size can be related to the number of interconnected sheets and edges with more sheets creating

smaller cavities, consistent with a previous report [21]. Moreover, The ZnAl-LDHs films on the Al plate at 200 and 250 °C revealed needle-like morphology (Fig. 3d-e). These needle shapes illustrated a compact and regular crystal structure with sharp-pointed needle-like edges. All SEM analyses demonstrated that the ZnAl-LDHs films grown on the Al plate are constituted by frameworks of interconnected ZnAl-LDHs sheets with thicknesses of approximately 100-250 nm. Furthermore, no extra metal particles or impurities were observed in the ZnAl-LDHs films [22].

The elemental mapping with EDX was performed to verify the distribution of elements in the region of ZnAl-LDHs films coated on the Al plate, as shown in Fig. 4. The surface films of ZnAl-LDHs showed the distribution of characteristic spots for zinc (Zn, orange), aluminum (Al, yellow) and oxygen (O, blue), which accounted for 13.70 and 30.87 % by mass for a strong signal from Zn and Al atoms, respectively, corresponding to the general formula $[(Zn_{1-x}Al_x)^{2+}(OH)_2]^{x+}(NO_3^-)(CO_3^{2-}) \cdot mH_2O$ of the ZnAl-LDHs films.

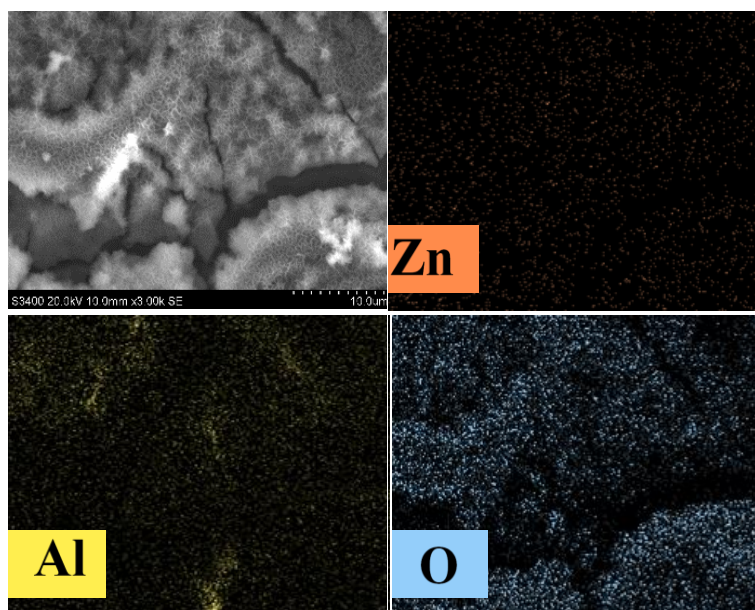


Fig. 4. EDX mapping of the ZnAl-LDHs films coated on the Al plate.

XRD technique was used to characterize the crystal structure, as shown in Fig. 5. In the diffractograms, one diffraction (*) at 38.50° was observed which matched the (111) reflections of the c-Al plane (JCPDS No. 04-0787), associated with the metal Al substrate [21]. An intense diffraction pattern of the ZnAl-LDHs films on the Al plate at 120, 150 and 200 °C showed 2θ values (°) at around 9.94-10.33, 19.92-20.36 and 34.38-34.88° which indicated the (003), (006) and (012) planes of a crystalline in a rhombohedral symmetry of the layered double hydroxide (LDHs) phase which was mainly composed of ZnAl-hydrotaalcite structure (JCPDS No. 38-0486) in good agreement with a previous report [23]. Moreover, a set of diffractions at 31.54 and 36.76° was identified as the (110) and (101) reflection planes of the hexagonal wurtzite ZnO structure (Δ) in good consistence with the studied data (JCPDS No. 36-1451) [18]. However, XRD patterns of the sample coated on the Al plate at 250 °C showed only ZnO structure. Additionally, the peaks at 9.94-10.33° showed a shoulder, which indicated the presence of anionic species (NO_3^- and CO_3^{2-}) in the interlayer space of the ZnAl-LDHs structure [24]. Furthermore, the XRD peaks became prominent with the reaction temperature which was attributed to the growth of thicker ZnAl-LDH films. Therefore, these results confirmed that the ZnAl-LDHs were synthesized and coated on Al plates.

The chemical interactions between ZnAl-LDHs and the Al plate are crucial to the chemical properties of the ZnAl-LDHs-coated on the Al plate. The FTIR spectra of the Al plate and the ZnAl-LDHs-coated on the Al plate by the hydrothermal method at various temperatures

are shown in Fig. 6. The FTIR spectra of all samples showed strong and broad absorption peaks at around 3368 cm^{-1} attributed to the O-H stretching in the LDH layers [25]. The characteristic peaks observed around 1645 cm^{-1} were assigned to the O-H bending of interlayer water molecules and brucite sheet. The stronger absorption peak at 1344 cm^{-1} for the $150\text{ }^{\circ}\text{C}$ sample corresponded to the stretching mode of the interlayer nitrate (NO_3^-) and carbonate anions (CO_3^{2-}) in the symmetric environment of the ZnAl-LDHs [26]. The absorption peaks at 779 cm^{-1} was attributed to the deformation mode of Al-OH and Zn-OH, whereas that at 663 cm^{-1} was assigned to the ZnO [27]. These absorption bands confirmed the formation of the ZnAl-LDHs characteristic phase, consistent with their XRD results [25, 28, 29]. The optimum temperature for preparing the ZnAl-LDH films via the hydrothermal method was found to be $150\text{ }^{\circ}\text{C}$ due resulting in the pure LDHs structure. These results confirmed that the ZnAl-LDHs films were successfully coated on the Al plate.

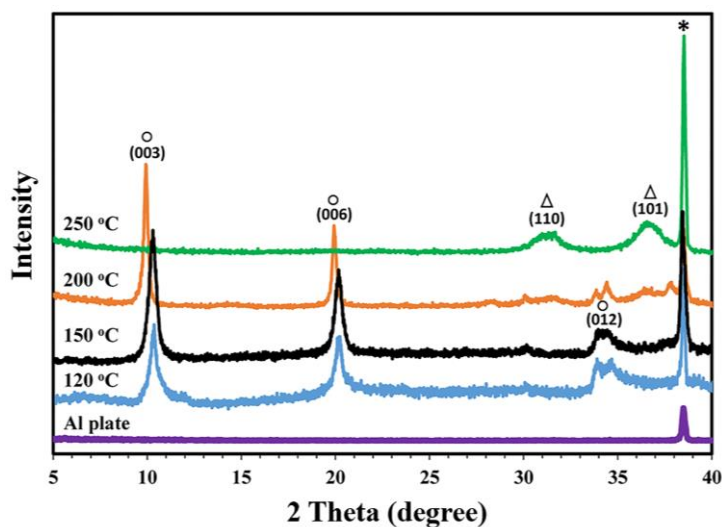


Fig. 5. XRD patterns of the ZnAl-LDHs films on the Al plate via the hydrothermal process at various temperatures.

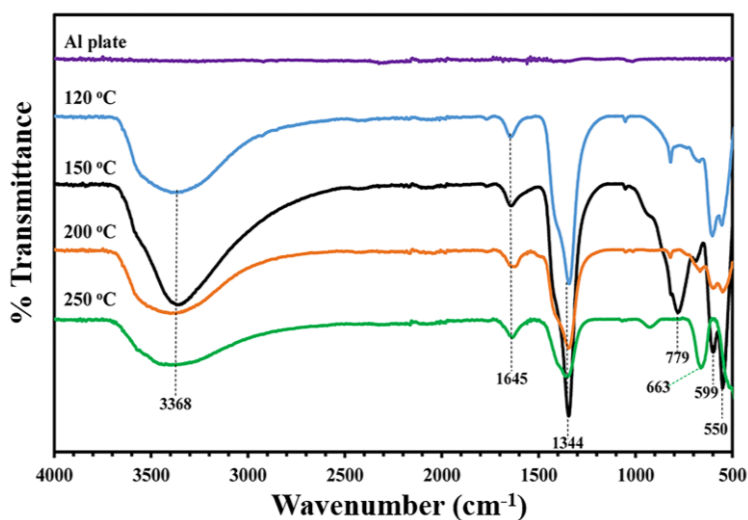


Fig. 6. FTIR spectra of the ZnAl-LDHs-coated on the Al plate by the hydrothermal method at various temperatures.

3.2. Adsorption properties

To assess the potential application of the as-prepared ZnAl-LDHs films on Al plates for the removal application in wastewater treatment, the OII dye was used as the target model to observe the efficiency in adsorption. This experiment was carried out at room temperature. Fig. 7 represents the removal of OII dye by using ZnAl-LDHs prepared at various temperatures. The following OII dye removal efficiency was observed: 250C-ZnAl LDHs > 200C-ZnAl LDHs > 150C-ZnAl LDHs > 120C-ZnAl LDHs, respectively. The above order of dye removal for dye concentrations of 200 ppm and 600 ppm can be explained as follows. High temperature treatment changed the ZnAl-LDHs crystallinity and thus significantly improved the surface area and porosity which acted as the active site for dye removal. The SEM images proved that the needle-like ZnAl-LDH was more formed and gave greater removal efficiency against the dye. Higher temperature may also convert LDH to the layered double oxide (LDO) form [30] with some portion of ZnO. However, at this point the removal efficiency did not gain better benefit as observed in the 600 ppm OII experiment, and the cost of temperature operation is considered wasteful.

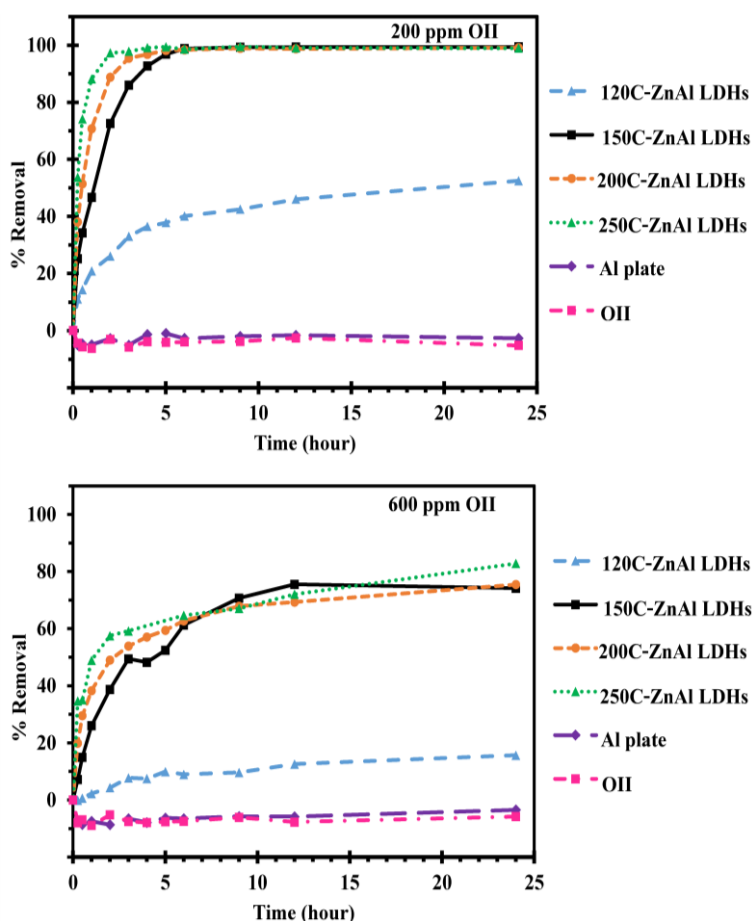


Fig. 7. Comparison of the removal efficiencies of OII by using ZnAl-LDHs at various temperatures

According to Fig. 8 in which OII dye and the OII dye-adsorbed on ZnAl-LDHs are comparatively studied in terms of FTIR spectra. The vibrational absorption of the new peaks due to the C=C stretching of the naphthalene and benzene rings from OII dye at 1612 and 1513 cm^{-1} could be observed in the OII dye-adsorbed ZnAl-LDHs spectra while the 1450 cm^{-1} corresponding to its N=N signal is observed as a small peak [31]. FTIR peaks of the vibration band of OII groups slightly shifted towards lower frequencies which confirmed the fixation of the dye at these sites on the surface of the ZnAl-LDHs. After exchange of anions, the possible adsorption of OII dye onto

the ZnAl-LDHs could be mainly due to chemisorption (ionic bond formation) between the Al^{3+} cation and the negatively charged OII ($-\text{SO}_3^-$) [23].

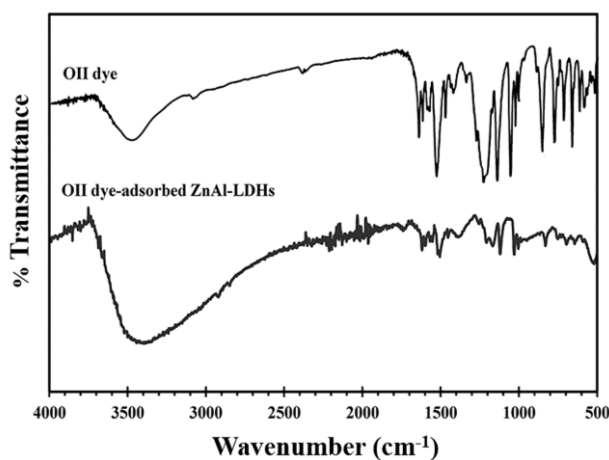


Fig. 8. FTIR spectra of the orange II (OII) dye and OII dye-adsorbed on ZnAl-LDHs.

The adsorption mechanism could be explained by the interaction between OII dye and the surface of the ZnAl-LDHs (Fig. 9). The possible interaction mechanisms of OII involved electrostatic attraction by the positive surface of ZnAl-LDHs and anion exchange with the interlayer anions [32].

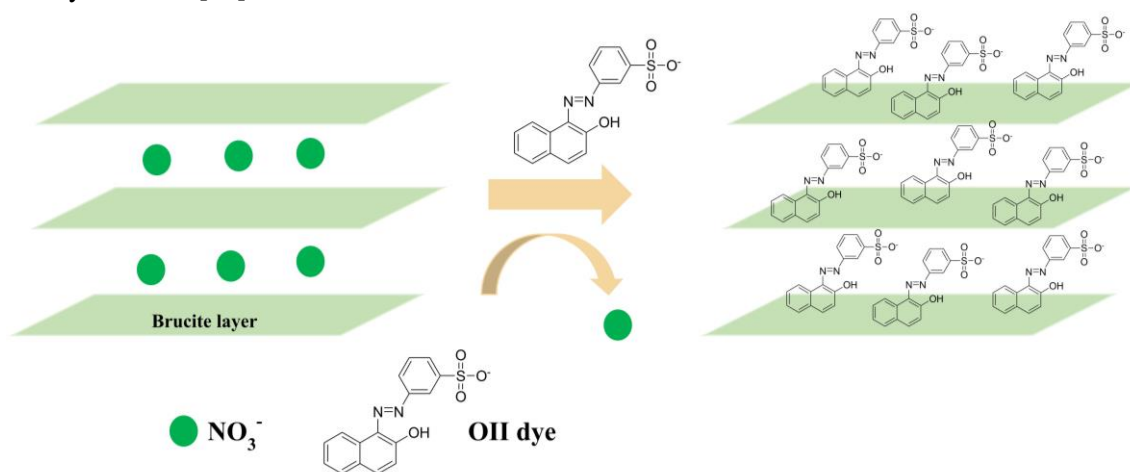


Fig. 9. Proposed adsorption mechanism of the OII adsorbed on ZnAl-LDHs.

4. Conclusions

ZnAl-LDH films were successfully prepared by the hydrothermal technique. The SEM images showed that the ZnAl-LDH films with hierarchical nanoarchitectures were fabricated on the surface of the aluminum substrates. EDX analysis of the ZnAl-LDH films revealed that Zn, Al, and O were dispersed on the aluminum substrates. XRD results showed that the ZnAl-LDH films were mainly composed of ZnAl-hydrotralcites structure. The FTIR spectra showed the characteristic band of bending vibrations of interlayer water, stretching vibrations of carbonate anion and nitrate anion in the interlayer, O-H bending of interlayer water molecules, brucite sheet and lattice vibrations of Zn-O. The removal of orange II dye using the as-prepared LDHs showed high sorption ability. The optimum temperature for preparing the ZnAl-LDH films via the hydrothermal method was found to be 150 °C resulting in the pure LDHs structure. The

hierarchically porous ZnAl-LDH films, with tunable morphology and low toxicity, is a promising adsorbent for the removal of organic contaminants from wastewater.

Acknowledgements

The author would like to thank the Faculty of Science, Silpakorn University, Nakhon Pathom, Thailand for financial support (Grant No. SRIF-JRG-2563-14).

References

- [1] C. Wang, A. Yediler, D. Lienert, Z. Wang, A. Kettrup, *Chemosphere* 46(2), 339 (2002); [https://doi.org/10.1016/S0045-6535\(01\)00086-8](https://doi.org/10.1016/S0045-6535(01)00086-8)
- [2] M. A. Rauf, M. A. Meetani, S. Hisaindee, *Desalination* 276(1), 13 (2011); <https://doi.org/10.1016/j.desal.2011.03.071>
- [3] Momina, M. Rafatullah, S. Ismail, A. Ahmad, *Water* 11(6), 1304 (2019); <https://doi.org/10.3390/w11061304>
- [4] M. M. Oktriyanti, N. R. Palapa, R. Mohadi, A. Lesbani, *Indonesian Journal of Environmental Management and Sustainability* 3(3), 93 (2019).
- [5] N. R. Palapa, R. Mohadi, A. Rachmat, A. Lesbani, *Mediterranean Journal of Chemistry* 10(1), 33 (2020); <https://doi.org/10.13171/mjc10102001261236al>
- [6] Z. Huang, T. Wang, M. Shen, Z. Huang, Y. Chong, L. Cui, *Chemical Engineering Journal* 369, 784 (2019); <https://doi.org/10.1016/j.cej.2019.03.136>
- [7] C. Suwanchawalit, S. Buddee, S. Wongnawa, *Journal of Environmental Sciences* 55, 257 (2017); <https://doi.org/10.1016/j.jes.2016.04.030>
- [8] S. Buddee, C. Suwanchawalit, S. Wongnawa, *Digest Journal of Nanomaterials and Biostructures* 12, 829 (2018).
- [9] Z. Noorimotlagh, S. A. Mirzaee, S. S. Martinez, S. Alavi, M. Ahmadi, N. Jaafarzadeh, *Chemical Engineering Research and Design* 141(1), 290 (2019); <https://doi.org/10.1016/j.cherd.2018.11.007>
- [10] G. K. Sarma, S. Sen Gupta, K. G. Bhattacharyya, *SN Applied Sciences* 1(3), 211 (2019); <https://doi.org/10.1007/s42452-019-0216-y>
- [11] O. Segun Esan, A. Olaniran Kolawole, A. Christopher Olumuyiwa, *American Journal of Polymer Science and Technology* 5, 16 (2019); <https://doi.org/10.11648/j.ajpst.20190501.13>
- [12] Z. Yang, F. Wang, C. Zhang, G. Zeng, X. Tan, Z. Yu, Y. Zhong, H. Wang, F. Cui, *RSC Advances* 6(83), 79415 (2016); <https://doi.org/10.1039/C6RA12727D>
- [13] G. George, M. P. Saravanakumar, *Environmental Science and Pollution Research* 25(30), 30236 (2018).
- [14] H. Zhang, H. Chen, S. Azat, Z.A. Mansurov, X. Liu, J. Wang, X. Su, R. Wu, *Journal of Alloys and Compounds* 768, 572 (2018); <https://doi.org/10.1016/j.jallcom.2018.07.241>
- [15] M. Szabados, Z. Kónya, Á. Kukovecz, P. Sipos, I. Pálkó, *Applied Clay Science* 174(1), 138 (2019).
- [16] J. Wang, T. Zhang, M. Li, Y. Yang, P. Lu, P. Ning, Q. Wang, *RSC Advances* 8(40), 22694 (2018).
- [17] B. Wan, Y. Yan, R. Huang, D.B. Abdala, F. Liu, Y. Tang, W. Tan, X. Feng, *Science of The Total Environment* 650(1), 1980 (2019); <https://doi.org/10.1016/j.scitotenv.2018.09.230>
- [18] K. Dutta, S. Das, A. Pramanik, *Journal of Colloid and Interface Science* 366(1), 28 (2012); <https://doi.org/10.1016/j.jcis.2011.09.081>
- [19] O. O. Balayeva, *Journal of Dispersion Science and Technology*, 1 (2021); <https://doi.org/10.1080/01932691.2020.1848580>
- [20] A. A. Matin, P. Biparva, H. Amanzadeh, K. Farhadi, *Talanta* 103(1), 207 (2013);

<https://doi.org/10.1016/j.talanta.2012.10.034>

- [21] M. S. Pedraza-Chan, U. Salazar-Kuri, R. Sánchez-Zeferino, I. I. Ruiz-López, A. Escobedo-Morales, *Applied Clay Science* 210(1), 106159 (2021); <https://doi.org/10.1016/j.clay.2021.106159>
- [22] S. Jamil, S. R. Khan, A. R. Alvi, F. Kausar, S. Ali, S. A. Khan, M. Naim, A. Malik, M. R. S. A. Janjua, *Chemical Physics* 528(1), 110530 (2020); <https://doi.org/10.1016/j.chemphys.2019.110530>
- [23] H. Ouassif, E. M. Moujahid, R. Lahkale, R. Sadik, F. Z. Bouragba, E. M. Sabbar, M. Diouri, *Surfaces and Interfaces* 18(1), 100401 (2020); <https://doi.org/10.1016/j.surfin.2019.100401>
- [24] M. Yasaei, M. Khakbiz, E. Ghasemi, A. Zamanian, *Applied Surface Science* 467-468(1), 782 (2019); <https://doi.org/10.1016/j.apsusc.2018.10.202>
- [25] J. Liu, J. Song, H. Xiao, L. Zhang, Y. Qin, D. Liu, W. Hou, N. Du, *Powder Technology* 253(1), 41 (2014); <https://doi.org/10.1016/j.powtec.2013.11.007>
- [26] K.-H. Goh, T.-T. Lim, Z. Dong, *Water Research* 42(6), 1343 (2008); <https://doi.org/10.1016/j.watres.2007.10.043>
- [27] A. Kołodziejczak-Radzimska, E. Markiewicz, T. Jesionowski, *Journal of Nanomaterials* 2012, 656353 (2012); <https://doi.org/10.1155/2012/656353>
- [28] Y. Feng, D. Li, Y. Wang, D. G. Evans, X. Duan, *Polymer Degradation and Stability* 91(4), 789 (2006); <https://doi.org/10.1016/j.polymdegradstab.2005.06.006>
- [29] S. Ma, C. Fan, G. Huang, Y. Li, X. Yang, K. Ooi, *European Journal of Inorganic Chemistry* 14, 2079 (2010); <https://doi.org/10.1002/ejic.201000010>
- [30] X. Fang, C. Chen, H. Jia, Y. Li, J. Liu, Y. Wang, Y. Song, T. Du, L. Liu, *Journal of Industrial and Engineering Chemistry* 95, 16 (2021); <https://doi.org/10.1016/j.jiec.2020.12.027>
- [31] H. Umukoro, M. G. Peleyeju, J. C. Ngila, O. A. Arotiba, *Chemical Engineering Journal* 317, 290 (2017); <https://doi.org/10.1016/j.cej.2017.02.084>
- [32] E. D. Isaacs-Paez, R. Leyva-Ramos, A. Jacobo-Azuara, J. M. Martinez-Rosales, J. V. Flores-Cano, *Chemical Engineering Journal* 245, 248 (2014); <https://doi.org/10.1016/j.cej.2014.02.031>